Journal of Power Sources 182 (2008) 558–564

Contents lists available at ScienceDirect

Journal of Power Sources

journal homepage: www.elsevier.com/locate/jpowsour

Fast and exergy efficient start-up of micro-solid oxide fuel cell systems by using the reformer or the post-combustor for start-up heating

Michael J. Stutz [a], Robert N. Grass [b], Stefan Loher [b], Wendelin J. Stark [b], Dimos Poulikakos [a,*]

[a] Laboratory of Thermodynamics in Emerging Technologies, Institute of Energy Technology, Department of Mechanical and Process Engineering, ETH Zurich, Sonneggstrasse 3, CH-8092 Zurich, Switzerland

[b] Functional Materials Laboratory, Institute for Chemical and Bioengineering, Department of Chemistry and Applied Biosciences, ETH Zurich, CH-8092 Zurich, Switzerland

ARTICLE INFO

Article history:
Received 16 January 2008
Received in revised form 7 April 2008
Accepted 9 April 2008
Available online 2 June 2008

Keywords:
Start-up
Heat source
Micro-SOFC
Rhodium
Reformer
Post-combustor

ABSTRACT

The start-up process of a micro-solid oxide fuel cell system strongly influences its overall efficiency, especially for portable applications where a frequent switch-on and switch-off is required. We present herein a novel start-up process for such systems that exploits existing units, such as the post-combustor or the reformer, as a heat source to reach the operation temperature of the cell at 600 °C. Our experimental results show that the employment of platinum catalysts in the post-combustor or rhodium catalysts in the reformer for total oxidation of butane by air combined with an electrically heated wire led to a faster and more efficient start-up than conventional start-up methods using only electrical energy. By using the post-combustor as heat source, the start-up time could be reduced by 79% and the exergy cost by 86%. The latter includes the cost of the stand-alone fuel cell system to produce electrical energy for the joule heating of the wire (i.e. the system efficiency is accounted for). There are several advantages to use the reformer as heat source during start-up, such as prevention of coking of the fuel cell or improved heat transfer by internal heating of the other components. The start-up performance, however, was lower than that of the post-combustor: the start-up time could be reduced by 65% and the exergy cost by 68% compared to a conventional start-up.

1. Introduction

Micro-fuel cell systems are known as a promising alternative for power generation for portable applications including the field of consumer electronics (mobile phones, notebooks, camcorders, etc.), medical and health care devices, and industrial applications (handheld scanners, portable data collectors, etc.) [1]. Recent studies showed that especially micro-solid oxide fuel cells (μSOFC) show a high potential due to the high power density of the fuel cell [2,3] and excellent partial oxidation abilities of the reformer [4–6]. However, such systems operate at rather high temperatures leading to challenges in material science and thermal management [7]. Thus, several investigations on temperature reduction down to 500–700 °C were performed [8,9].

The start-up of such a system is an important issue to address, not only to make it fast, but also exergetically efficient [10], especially for portable applications, where a frequent switch-on and switch-off is required. This also leads to challenges in material properties due to thermal cycling, which can be addressed by applying thin film techniques [3]. Butane was chosen as fuel due to its efficient storage capability in cartridges. Hotz et al. [11] optimized a whole μSOFC system from the exergetic point of view. They showed that electrical power production generates losses in most subunits of such a system. By optimization, a maximum exergetic efficiency of 0.19 at 600 °C is considered realistic. However, the transient start-up process was not investigated. Thus, if the entire exergy in the start-up process is provided through electrical power, the losses to produce the electrical exergy leading to an exergetic inefficient start-up method have to be included. It is therefore more reasonable to convert chemical exergy stored in the fuel tank directly into heat. Schmidt et al. [12] showed that this can be done by homogeneous combustion initiated by an ignition spark in a separate chamber lying in front of the devices that need to be heated up. The drawback is that this method can generate very high temperatures unsuitable for μSOFC applications. Jung et al. [13] presented a start-up method where the metallic monolith, which acted as mechanical support, was electrically heated up to the operation temperature for partial oxidation of methane. The entire exergy was provided by an electrical source. Another interesting start-up method employs the catalytic activity of hydrogen on platinum at room temperature to start-up a fuel cell system [14]. The hydrogen needed for the heat-up process stems from a hydrogen buffer, which is refilled in normal

* Corresponding author. Tel.: +41 44 632 2435; fax: +41 44 632 1176.
E-mail address: dimos.poulikakos@ethz.ch (D. Poulikakos).

0378-7753/$ – see front matter © 2008 Elsevier B.V. All rights reserved.
doi:10.1016/j.jpowsour.2008.04.020

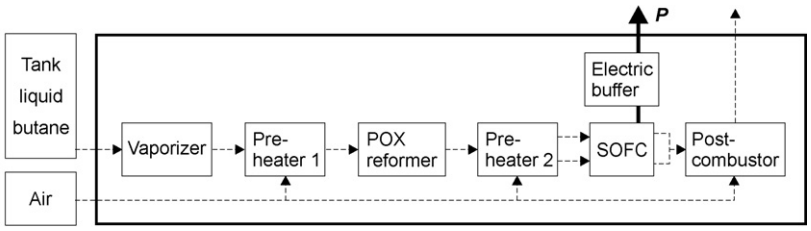

Fig. 1. Schematic of a μSOFC system adapted from Hotz et al. [11]. Mass flows (- - -) and electric power output *P* are shown.

operation by the fuel reformer. The disadvantage of that system lies in the complicated purification process of the reformate gas for the hydrogen buffer, the difficult hydrogen storage and the rather complex tubing of the system.

Simplicity is an important factor in micro-systems and therefore it is of a big advantage, if existing system components are exploited for the optimization of the start-up process. The straightforward solution is to use the post-combustor of a μSOFC system (Fig. 1) to convert chemical exergy to heat by total oxidation [15]. The main task of this component is to totally oxidize the harmful gases at the fuel cell outlet, which are either toxic (e.g. CO) and/or explosive (e.g. H_2, hydrocarbons). Thus, the catalyst is already adapted for total oxidation.

Recently, Lee et al. [16] showed the capability of rhodium, which was primarily employed as partial oxidation or steam reforming catalyst, for total oxidation of propane. Hence, such a reformer also shows excellent partial oxidation performance if flame-made rhodium nanoparticles are employed [4] and can also be exploited as heat source by total oxidation of fuel. By using the reformer as a heat generator during the start-up, several advantages arise: totally oxidized, hot combustion gases leaving the reformer directly enter other units of the μSOFC system and heat them from the inside (Fig. 1). By using the post-combustor as heat source, the other components can only be heated indirectly via a heat exchanger heating the inflow gases or by conduction in the solid part. In terms of long-term performance, the decreased tendency towards coking of such a fuel cell is attractive, since coking and other deactivation mechanisms are a serious problem in fuel cell research, because they lower the performance of the fuel cell [17]. If the reformer is used as heat source, the fuel/air mixture is burnt before the inlet of the fuel cell. Thus, a harmless mixture of CO_2 and H_2O enters the fuel cell. In a system heated by the post-combustor, unburned or partially burned fuel flows through the fuel cell. The fuel cell temperature rises constantly during the start-up process. It is known that for certain mixtures with carbon contents (other than CO_2) and certain temperatures, deactivation of the fuel cell occurs by carbon deposition [18]. During start-up, it is likely that at least at one moment the condition inside the fuel cell is in the deactivation regime. Furthermore, the buffer volume defined as the volume between the fuel container and the reaction zone (reformer and post-combustor, respectively) of the hybrid design using the reformer as heat source is considerably smaller and can therefore be better controlled.

In this study, we experimentally investigated the start-up process of a μSOFC system by comparing two different hybrid systems to a conventional electric start-up process. The post-combustor or the reformer was used as heat source by catalytically converting butane and air. A heating wire brought the hybrid reactor to the ignition temperature. In the conventional reference set-up joule heating was used to bring the assembly to the operation temperature. Our study demonstrates the feasibility of these two more efficient hybrid systems. Furthermore, we expected a reduction of start-up time and exergy cost of the hybrid systems. The resulting short start-up time and high exergetic efficiency enables a frequent shut-down and start-up, which is crucial for most portable applications.

We deliberately kept the test rig as simple as possible but, at the same time, realistic enough to show the feasibility of the hybrid start-up method. In a real system, the heat transfer can be different than in our test rig. However, many parameters, such as the arrangement and the design of the units, the bonding between them and the material properties are not known a priori and can differ largely, which would make a quantitative prediction vague.

2. Experiments

2.1. Catalyst preparation

The $Ce_{0.5}Zr_{0.5}O_2$ nanoparticles with 2 wt.% rhodium doping by the one-step process flame spray synthesis were identical to those used in the study by Hotz et al. [4]. The $Ce_{0.5}Zr_{0.5}O_2$ nanoparticles with 1.6 wt.% platinum doping were prepared according to Stark et al. [19]. The only difference lay in the precursor for the catalyst support where we used cerium(III) 2-ethylhexanoate (12 wt.% Ce, Shepherd Chemical Company) and zirconium(IV) 2-ethylhexanoate (18 wt.% Zr, Borchers GmbH) with a metal concentration of 0.4 mol L^{-1} each [20].

2.2. Catalyst characterization

The characterization of the $Rh/Ce_{0.5}Zr_{0.5}O_2$ was measured previously by Hotz et al. [4]. The specific surface area and the phase composition of the platinum catalyst were measured according to the same study. The platinum content was measured after digestion of the catalyst in hydrochloric acid (37 wt.%, J.T. Baker, 1 week) by flame atomic adsorption spectroscopy (AAS) on a Varian SpectrAA 220FS (slit width 0.2 nm, lamp current 10.0 mA) applying a Air (13.5 L min^{-1}) acetylene (2 L min^{-1}) flame and measuring adsorption at a wavelength of 265.9 nm. The catalyst was further analyzed by transmission electron microscopy (CM30 ST, Philips, LaB6 cathode, operated at 300 kV, point resolution ~4 Å) after deposition of the particles onto a carbon foil supported on a copper grid.

2.3. Test setup for measurements of total oxidation capability of catalysts

The test setup to investigate the capability of the catalyst to totally oxidize butane and air [4] consisted of a packed bed containing 22.5 mg purified and calcined SiO_2 sand (Riedel-deHaën, average diameter: 0.2 mm) mixed with 7.5 mg $Rh/Ce_{0.5}Zr_{0.5}O_2$ nanoparticles (2.0 wt.% Rh) or with 7.5 mg $Pt/Ce_{0.5}Zr_{0.5}O_2$ nanoparticles (1.6 wt.% Rh). The porous packed beds were fixed in the Inconel tube between ceramic fiber plugs consisting of SiO_2 and Al_2O_3. The catalytic effect of the Inconel tube on the reactions was shown to be negligible by comparing it with a fused silica tube [4]. As a reference, a packed bed of 30 mg SiO_2 sand was prepared.

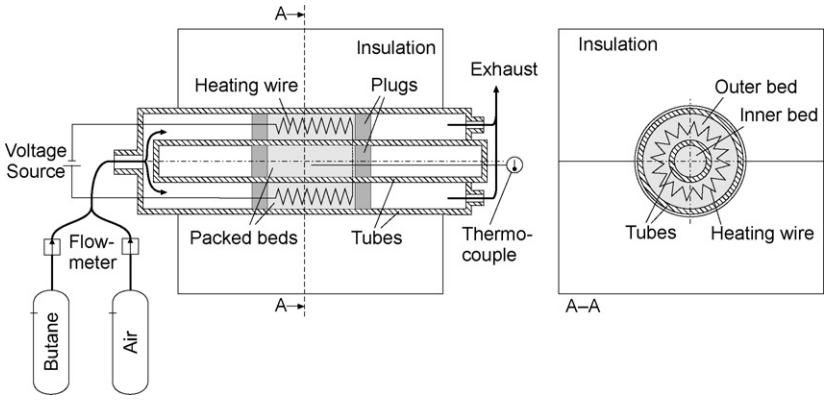

Fig. 2. Schematic of the test rig for the start-up experiments with cross-section (A–A).

We used the test rig according to Hotz et al. [4] with constant air and butane inlet flow rates of 21.0 mL min^{-1} and 0.65 mL min^{-1}, respectively, leading to mole fractions of $X_{C_4H_{10}} = 3.1\%$, $X_{O_2} = 20.3\%$, and $X_{N_2} = 76.6\%$. This corresponds to the stoichiometric fuel to air ratio, based on total oxidation and similar residence times as in the start-up experiments. Air is assumed as an ideal gas, butane density is calculated by the Benedict–Webb–Rubin equation for light hydrocarbons [21]. The entire reactor was heated under constant air/butane flow. The molar composition of the outlet gas was determined by a GC/MS described by Hotz et al. [4]. The molar product gas balance of carbon closed within 5%.

2.4. Test setup for start-up measurements

The test rig consisted of two concentric tubes (fused silica) enclosing two packed beds (Fig. 2). The outer packed bed (length: 10 mm) was fitted between the outer (inner diameter: 4.9 mm, outer diameter: 7.0 mm) and the inner tube (inner diameter: 1.6 mm, outer diameter: 3.0 mm). It consisted of 90 mg purified and calcined SiO_2 sand (Riedel-deHaën, average diameter: 0.2 mm) mixed with 30 mg $Pt/Ce_{0.5}Zr_{0.5}O_2$ or with 30 mg $Rh/Ce_{0.5}Zr_{0.5}O_2$ nanoparticles. We filled the inner tube in a similar fashion (22.5 mg SiO_2 sand mixed with 7.5 mg $Rh/Ce_{0.5}Zr_{0.5}O_2$ nanoparticles) building a readily usable packed bed reactor (length: 10 mm). It thermally represents the presence of other components of the μSOFC system, such as the reformer or the post-combustor, respectively. The plugs made of ceramic fiber paper (SiO_2 and Al_2O_3) kept the packed beds in place. A resistance heating wire (ferritic alloy, 73.2% Fe, 22% Cr and 4.8% Al, Kanthal D from Sandvik AB, diameter: 0.2 mm, length: 80 mm) was bent several times and embedded inside the outer packed bed. It was connected to a voltage source by two enameled copper wires (diameter: 0.2 mm, Rowan Products Ltd.). The test rig was insulated by two identical cuboidal halves (100 mm × 100 mm × 50 mm, WDS ultra from Porextherm Daemmstoffe GmbH, thermal conductivity of 0.018 W m^{-1} K^{-1} at 50 °C varying to 0.031 W m^{-1} K^{-1} at 600 °C) featuring a half tubular cut-out (7 mm diameter) in order to totally enclose the outer tube along a length of 100 mm. The tubing from the reactor outlet to the exhaust was heated in order to avoid clogging by condensed water. The temperature was measured by a thermocouple (K type, diameter: 0.5 mm) inside the inner packed bed. Therefore, the heat transfer from the heating zone to the other components of the fuel cell system was accounted for. In order to minimize the heat loss by conduction, the number of thermocouples that measure the temperature inside the hot zone was minimized. Thus, we decided to use only one thermocouple that measured the center part of the reactor, i.e. the packed bed of the inner tube. Rough estimations, by considering only heat conduction in the axial direction, showed that the addition of a second thermocouple would decrease the thermal resistance by 24%. The placement of the thermocouple in the outer tube was not possible, because it would have interfered with the electrical heating wire.

For the hybrid start-up process the following procedure was applied:

- *Step 1*: application of a constant voltage in heating resistance and simultaneous introduction of a butane/air mixture to the test unit [4] in a stoichiometric fuel to air ratio, based on total oxidation. The air and butane inlet flow rates were constant at 122.3 mL min^{-1} and 3.8 mL min^{-1} (at 1 atm and 0 °C), respectively. This leads to a possible maximum heat release based on total oxidation of butane and air (lower heating value) of 7.8 W.
- *Step 2*: when the temperature reached the stopping temperature, which is a variable system parameter, the voltage source was turned off.
- *Step 3*: at T = 600 °C (operation temperature) the experiment ends. The time to reach the operation temperature is the start-up time t_1.

In this study, we chose the starting temperature of 40 °C. We used two different reactors: the first, containing the platinum catalyst in the outer tube, represented the start-up process of the μSOFC system if the post-combustor was used as heat source, the second, containing the rhodium catalyst in the outer tube simulated the start-up process, if the reformer was used as heat source.

As a reference measurement (i.e. the conventional start-up) we employed the same test rig with the following procedure:

- *Step 1*: application of a constant voltage in heating resistance. No mass flux (of an inert gas) is applied in order to avoid convective heat loss.
- *Step 2*: at T = 600 °C (operation temperature) the experiment ends. The time to reach the operation temperature is the start-up time t_1.

3. Results

3.1. Catalyst characterization

As previously shown by Stark et al. [19] flame spray pyrolysis can be used for the synthesis of stable ceria/zirconia supported platinum catalysts in a one-step process. The transmission electron micrograph of the as-prepared powder (Fig. 3) shows highly crystalline nanoparticles in the size range of 10–20 nm. The presence of

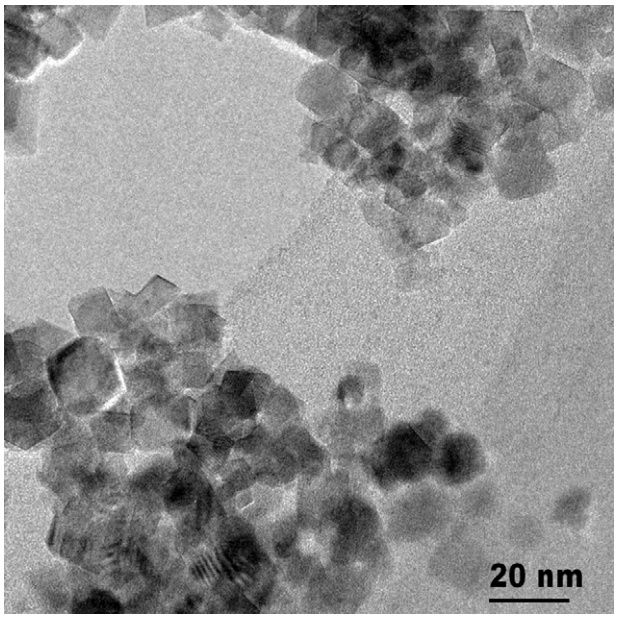

Fig. 3. Electron micrograph of flame-made 1.6 wt.% $Pt/Ce_{0.5}Zr_{0.5}O_2$ showing regularly shaped nanoparticles of around 10–20 nm diameter and narrow particle size distribution. The platinum is well dispersed on the support surface and not discernible by TEM [19].

nanocrystalline ceria/zirconia particles stays in agreement with the broad peaks of the X-ray diffraction pattern (Fig. 4) and confirms the material composition. The average particle size can be calculated from the material specific surface area (SSA = 68 $m^2\ g^{-1}$) assuming equally sized spherical nanoparticles [22] and reads $d_p = 6/(\rho\,SSA)$. It was calculated as ~15 nm, which is in good agreement with the observations from electron microscopy (Fig. 3).

3.2. Total oxidation capability of catalysts

Butane conversion is defined as the ratio between converted butane and inlet butane and describes the activity of a catalyst towards total oxidation of butane. Fig. 5 shows that the platinum catalyst already starts to convert butane (>5% conversion) at 180 °C and yielded 100% butane conversion at 260 °C. The rhodium catalyst showed a lower butane conversion at all measured temperatures. Its total oxidation activity started at around 220 °C. A high activity (84%) was obtained at 380 °C and further increased to 100% at 540 °C. A reference reactor with no catalyst started to convert butane at around 460 °C. At 540 °C, the butane conversion is still below 10%.

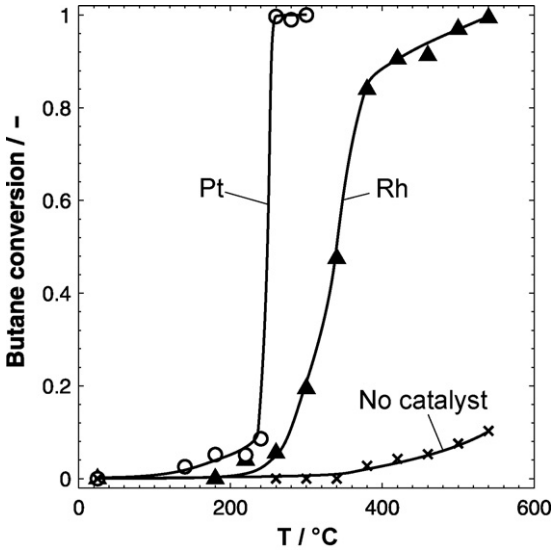

Fig. 5. Butane conversion as functions of reactor temperature for packed bed reactors with the platinum and rhodium catalyst and a reference without catalyst. The solid lines through the data points are curve fits.

3.3. Start-up dependent on electrical power input

The temperature profile of the hybrid start-up method for three different electrical power inputs is shown in Fig. 6. The slope of the three curves is similar above the stopping temperature (T_{stop} = 300 °C) where only total oxidation provides heat. Below the stopping temperature and for low power inputs, a kink in the curve

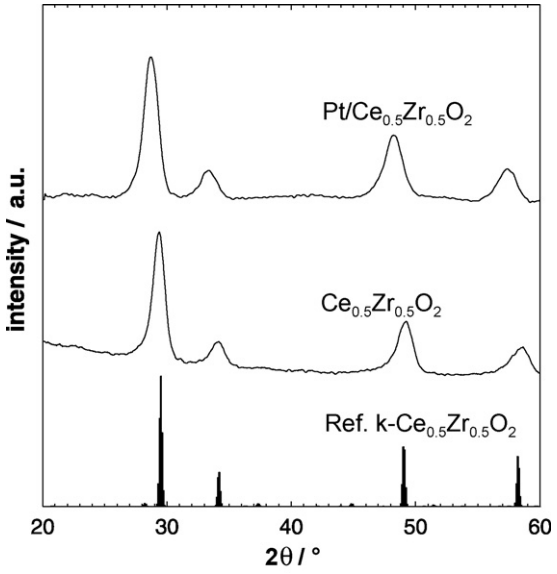

Fig. 4. X-ray diffraction pattern of as-prepared 1.6 wt.% $Pt/Ce_{0.5}Zr_{0.5}O_2$, $Ce_{0.5}Zr_{0.5}O_2$ [4] and reference κ-$Ce_{0.5}Zr_{0.5}O_2$ sample [26].

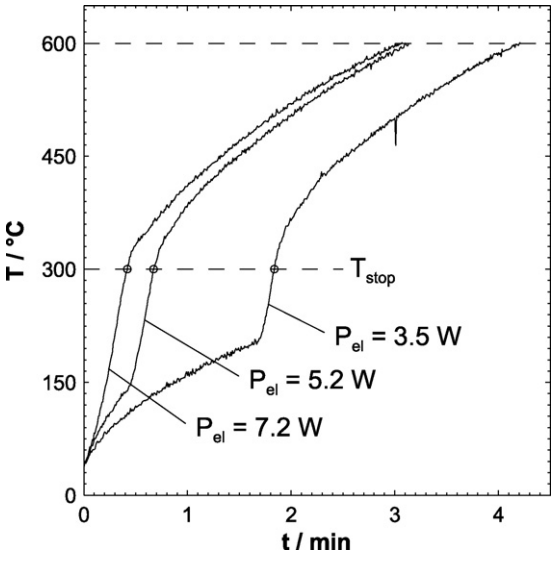

Fig. 6. Reactor temperature as functions of time for the hybrid start-up with the platinum catalyst for three different electrical power inputs. The stopping time is constant at 300 °C.

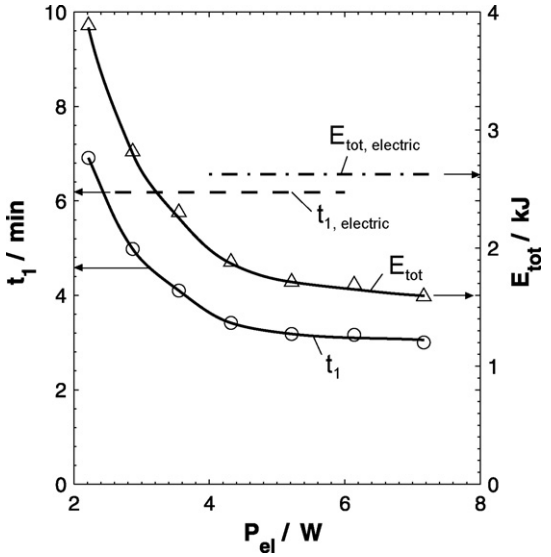

Fig. 7. Start-up time t_1 and total energy input E_{tot} of the hybrid start-up as functions of the mean electrical power input with a stopping temperature of 300 °C. Start-up time ($t_{1, electric}$) and total energy input ($E_{tot, electric}$) of the electric start-up. The solid lines through the data points are curve fits.

is clearly discernable. It is worth noting that the variation of electrical power input is below 2% for all experiments and therefore negligible.

The start-up time for the electrically heated reference system was about 6 min (Fig. 7) using a mean electrical power input of 7.1 W. We compared this value with a hybrid start-up method using a platinum catalyst and a stopping temperature of 300 °C. Using the same electrical power input (7.2 W) allowed a reduction of the start-up time by 51%. If the electrical power input is lowered, the start-up time also increases since the integral heat input required a longer heating period. It is worth noting that the mean electric power input can vary slightly, because it is the potential of the voltage source that we kept constant.

The integral heat input can be better represented by the total energy input E_{tot} as a function of the mean electrical power input. The total energy input in an improved hybrid system is defined as the inlet mass flux of butane times its lower heating value [21] plus the electrical energy input. A reference value (E_{tot} = 2.6 kJ) was derived from using only electrical power as the heat source. Fig. 7 shows that the total energy input could be reduced by 40% if the electrical power input is the same as in the reference measurement. For a lower electrical power input, the total energy input increased.

Since the largest reduction in start-up time and total energy requirement was found for a setup using the highest electrical power input, we chose this value for the following measurements. The maximum electrical power input was limited by the properties of the heating wire.

3.4. Start-up dependent on stopping temperature

In the following measurements the dependence of the start-up behavior versus stopping temperature was investigated for both the platinum and the rhodium catalyst. The start-up time for the rhodium catalyst was around 30 s longer than that of the platinum catalyst (Fig. 8a) for the reference catalyst. By varying the stopping temperature, the start-up time could be reduced by 79% for the platinum catalyst and by 65% for the rhodium catalyst for the highest stopping temperature (i.e. the operation temperature) of 600 °C. If we reduced the stopping temperature, the start-up time increased for both catalysts. However, the start-up time of the hybrid system is always markedly lower than that of the reference experiment. The lowest feasible stopping temperature for the platinum catalyst was 100 °C and yielded in a reduction of 47% compared to the reference value. If we applied a lower stopping temperature, the reactor was not able to reach the operation temperature. The lowest feasible stopping temperature for the rhodium catalyst was 300 °C resulting in a reduction of 29%.

For the reference experiments, the total energy input using a rhodium catalyst was slightly higher (2.9 kJ) than for a platinum catalyst (Fig. 8b). We obtained the highest reduction for the hybrid start-up if the stopping temperature was the highest, which was 55% for the platinum and 26% for the rhodium system. For lower stopping temperatures ($T_{stop} \leq 500$ °C) the total energy input did not vary strongly with temperature for both catalysts.

The total exergy cost can be defined as the total amount of exergy provided by the μSOFC system to reach operation temperature. The chemical exergy of butane $Ex_{TOX, butane}$ can be directly included into the total exergy cost. The electrical exergy Ex_{el}, however, must be produced from chemical exergy in a real stand-alone μSOFC system. The overall system efficiency has to be included in this analysis as chemical exergy cannot be converted to electrical exergy without significant losses. A previous study predicted a maximum exergetic efficiency of μ_{ex} = 0.19 for a μSOFC system operating at 600 °C

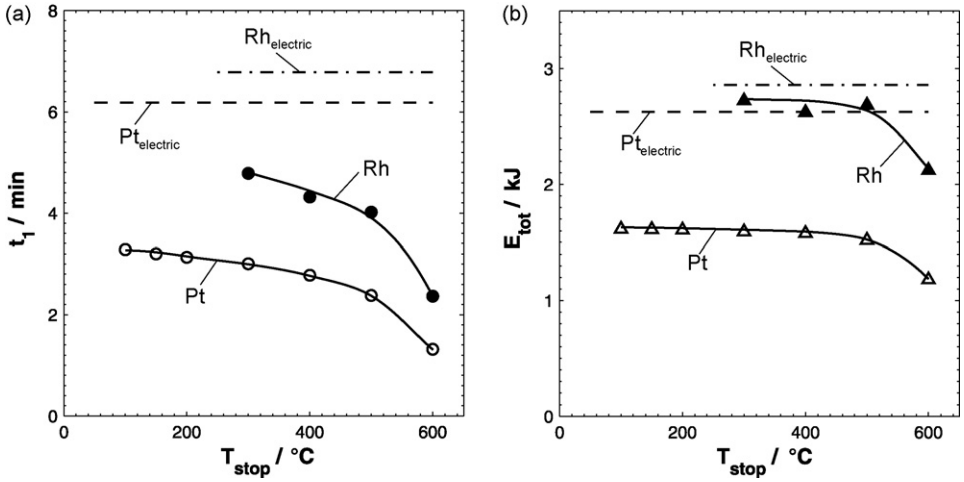

Fig. 8. Start-up time t_1 (a) and total energy input E_{tot} (b) of the hybrid start-up with the platinum and rhodium catalyst as functions of the stopping temperature T_{stop} and of the electric start-up with the platinum ($Pt_{electric}$) and rhodium catalyst ($Rh_{electric}$). The solid lines through the data points are curve fits.

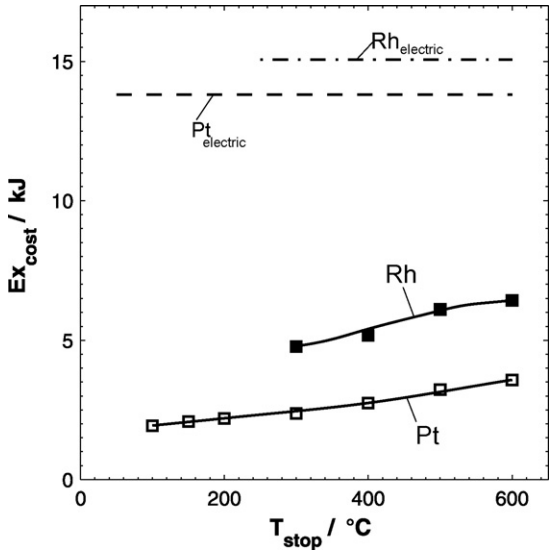

Fig. 9. Total exergy cost of the hybrid start-up process containing the platinum and rhodium catalyst as functions of the stopping temperature T_{stop} and of the electric start-up with the platinum ($Pt_{electric}$) and rhodium catalyst ($Rh_{electric}$). The solid lines through the data points are curve fits.

[11]. For simplicity, we neglected losses of storage and transport of electrical energy within the system. Thus, the total exergy cost reads:

$$Ex_{cost} = Ex_{TOX,\ butane} + \frac{Ex_{el}}{\mu_{ex}}. \quad (1)$$

The exergy provided by total oxidation of butane corresponds to the availability of liquid butane [23].

Fig. 9 shows that the total exergy cost for the reference start-up simulation in a μSOFC was 14 kJ for the platinum system and 15 kJ for rhodium. Maximum reduction for the platinum system was 74% and 57% for rhodium, if we applied the highest stopping temperature. However, the largest reduction could be achieved with the lowest stopping temperature. This was as high as 86% for the platinum system and 68% for the rhodium system.

4. Discussion

The present experiments confirm the excellent activity of platinum catalysts for total oxidation of butane and stay in good agreement to earlier studies [24]. The flame-made platinum catalyst was more active than the rhodium-based catalyst. Our results follow the findings of Lee et al. [16] who observed a high activity for rhodium on a different support. The present study shows that platinum is better suited for an integrated fuel cell design since the stopping temperature during start-up can be lowered to 100 °C.

Fig. 6 clearly shows that the heat input is similar for all cases above the stopping temperature, which is logic due to the same inlet mass flows. Thus, the inlet butane flow is totally converted. Below the stopping temperature, the curve can be divided into two parts: the first part where no total oxidation occurs and the second, steeper part that reflects the onset of the total oxidation.

The decrease of the start-up time with increasing electrical power input makes physically sense. The decrease in total energy input with increasing electrical power input, however, is not straightforward. In an ideally insulated system, the total energy input is independent of power input. In a real system a significant portion of heat is removed by convection or absorbed by the insulation. The present data show that for high electrical power output (P_{el} > 5 W) the assumption of perfect insulation is reasonable.

The here-observed differences between the start-up time of rhodium or platinum containing systems (9%) using only electricity for heating was within the acceptable limit. It does not stem from the different noble metals used but from the manufacturing process, such as the packing or the bending and embedding of the heating wire. The optimum operation conditions require a stopping temperature of 600 °C if the highest priority is minimal start-up time. We assume that the start-up time can be further decreased by increasing the butane/air mass flow thus increasing the chemical energy input. As stated above, the resistive heating wire has a certain limit concerning surface power load. Thus, a longer resistive wire with optimized coiling could provide a higher electrical power input. However, a very fast start-up possibly leads to a decrease in performance of the fuel cell [25].

The lowest feasible stopping temperature of the platinum reactor (Fig. 8) is surprising, since total oxidation activity only starts at considerably higher temperatures (Fig. 5). We conclude that locally inside the outer packed bed, the temperature must have reached the ignition temperature (hot spots). The lowest feasible stopping temperature of the platinum reactor is also lower than that of the rhodium reactor. This can be explained by the light-off of the platinum catalyst at a lower temperature.

The use of a hybrid start-up process led to large reductions of exergy cost for both rhodium- and platinum-based systems. The increase of exergy cost with increasing the stopping temperature can be explained with Eq. (1). The chemical exergy of butane Ex_{TOX} decreases with increasing stopping temperature, since the start-up time is longer (Fig. 8). Hence the exergy needed to electrically heat the wire is the dominant factor. It is worth noting that the optimum operation point is the lowest stopping temperature if the goal is to increase the exergetic efficiency, hence, the run time.

The results clearly showed that the use of a hybrid start-up process is advantageous if compared to a merely electrically heated system. We further showed that a hybrid start-up can be successfully applied using the post-combustor or the reformer for heating. The exergy cost reduction was higher for the platinum system. However, considering the other advantages explained above, the start-up with the reformer as heat source might be preferable.

5. Conclusions

The present work investigated the start-up process of a μSOFC system exploiting existing system units (reformer or post-combustor) as a catalytic reactor to convert butane and air to heat combined with an electrically heated wire. As a catalyst for the post-combustor we used flame-made $Pt/Ce_{0.5}Zr_{0.5}O_2$ nanoparticles and for the reformer $Rh/Ce_{0.5}Zr_{0.5}O_2$.

We showed that the operation temperature of 600 °C cannot only be reached significantly faster, but also in an exergetic more efficient way compared to the conventional start-up process, where only electrical energy is used.

By using the platinum catalyst as heat source the start-up time could be reduced up to 79% and the exergy cost up to 86%. Included in the latter is the overall μSOFC system efficiency to produce the electrical energy of the stand-alone micro-power plant. The results of the rhodium catalyst were also promising, though slightly weaker than those of the platinum catalyst. The start-up time could be reduced up to 65% and the exergy cost up to 68%. On the other hand, there are several advantages in using the reformer as heat source during start-up, such as direct heat transfer to the other components by convective internal heating and the prevention of coking of the fuel cell.

The ideal operation point is defined by a high electrical power input and a high stopping temperature (i.e. the operation temperature) if the goal is the start-up time reduction. For a high exergetic

efficiency the lowest possible stopping temperature defines the optimum operation point if a system with rapid response during start-up is designed.

Acknowledgements

We gratefully acknowledge the financial support by the following Swiss institutions: Commission for Technology and Innovation (CTI) (grants: KTI 7085.2 DCPP-NM and KTI 8446.1 DCPP-NM), Center of Competence Energy and Mobility (CCEM) and Swiss Electric Research.

References

[1] A.B. Bieberle-Hutter, D. Beckel, U.R. Muecke, J.L.M. Rupp, A. Infortuna, L.J. Gauckler, MST News 4 (2005) 12–15.
[2] Z.P. Shao, S.M. Haile, J. Ahn, P.D. Ronney, Z.L. Zhan, S.A. Barnett, Nature 435 (2005) 795–798.
[3] A.B. Bieberle-Hutter, D. Beckel, A. Infortuna, U.P. Muecke, J.L. Rupp, L.J. Gauckler, S. Rey-Mermet, P. Muralt, N.R. Bieri, N. Hotz, M.J. Stutz, D. Poulikakos, P. Heeb, P. Muller, A. Bernard, R. Gmür, T. Hocker, J. Power Sources 177 (2008) 123–130.
[4] N. Hotz, M.J. Stutz, S. Loher, W.J. Stark, D. Poulikakos, Appl. Catal. B: Environ. 73 (2007) 336–344.
[5] M.J. Stutz, N. Hotz, D. Poulikakos, Chem. Eng. Sci. 61 (2006) 4027–4040.
[6] M.J. Stutz, D. Poulikakos, Chem. Eng. Sci. 60 (2005) 6983–6997.
[7] L.J. Gauckler, D. Beckel, B.E. Buergler, E. Jud, U.R. Muecke, M. Prestat, J.L.M. Rupp, J. Richter, Chimia 58 (2004) 837–850.
[8] D. Beckel, U.P. Muecke, T. Gyger, G. Florey, A. Infortuna, L.J. Gauckler, Solid State Ionics 178 (2007) 407–415.
[9] J.L.M. Rupp, A. Infortuna, L.J. Gauckler, J. Am. Ceram. Soc. 90 (2007) 1792–1797.
[10] M.J. Stutz, W.J. Stark, D. Poulikakos, Method for starting up a fuel cell assembly, Patent EP07012131 (2007).
[11] N. Hotz, S.M. Senn, D. Poulikakos, J. Power Sources 158 (2006) 333–347.
[12] L.D. Schmidt, E.J. Klein, C.A. Leclerc, J.J. Krummenacher, K.N. West, Chem. Eng. Sci. 58 (2003) 1037–1041.
[13] H. Jung, W.L. Yoon, H. Lee, J.S. Park, J.S. Shin, H. La, J.D. Lee, J. Power Sources 124 (2003) 76–80.
[14] S.K. Ryi, J.S. Park, S.H. Cho, S.H. Kim, J. Power Sources 161 (2006) 1234–1240.
[15] D.A. Kearl, R.B. Peterson, K.D. Monte, Fuel cell using a catalytic combustor to exchange heat, US Patent 2004/0081871 (2004).
[16] A.F. Lee, C.R. Seabourne, K. Wilson, Catal. Commun. 7 (2006) 566–570.
[17] N.M. Sammes, R.J. Boersma, G.A. Tompsett, Solid State Ionics 135 (2000) 487–491.
[18] C.H. Bartholomew, Appl. Catal. A: Gen. 212 (2001) 17–60.
[19] W.J. Stark, J.D. Grunwaldt, M. Maciejewski, S.E. Pratsinis, A. Baiker, Chem. Mater. 17 (2005) 3352–3358.
[20] W.J. Stark, L. Madler, M. Maciejewski, S.E. Pratsinis, A. Baiker, Chem. Commun. (2003) 588–589.
[21] M.J. Moran, H.N. Shapiro, Fundamentals of Engineering Thermodynamics, 4th ed., John Wiley & Sons Ltd., Chichester, England, 2004.
[22] R.N. Grass, W.J. Stark, J. Mater. Chem. 16 (2006) 1825–1830.
[23] D.R. Morris, J. Szargut, Energy 11 (1986) 733–755.
[24] Y.F.Y. Yao, J. Catal. 87 (1984) 152–162.
[25] W. Bujalski, C.M. Dikwal, K. Kendall, J. Power Sources 171 (2007) 96–100.
[26] H. Kishimoto, T. Omata, S. Otsuka-Yao-Matsuo, K. Ueda, H. Hosono, H. Kawazoe, J. Alloy Compd. 312 (2000) 94–103.